



Effect of magnesium on dispersoid strengthening of Al–Mn–Mg–Si (3xxx) alloys

Zhen LI, Zhan ZHANG, X-Grant CHEN

Department of Applied Sciences, University of Québec at Chicoutimi,
555 boul. de l'Université, Saguenay, Québec, G7H 2B1, Canada

Received 6 May 2016; accepted 30 August 2016

Abstract: The effects of magnesium addition on the dispersoid precipitation as well as mechanical properties of 3xxx alloys were investigated. The microstructures in as-cast and heat-treated conditions were evaluated by optical microscopy and transmission electron microscopy. The results reveal that Mg has a strong influence on the distribution and volume fraction of dispersoids during precipitation heat treatment. The microhardness and yield strength at ambient temperature increase with increasing Mg content. The solid solution and dispersoid strengthening mechanisms of materials after heat treatment are quantitatively analyzed. Dispersoid strengthening for the alloys is the predominant strengthening mechanism after precipitation heat treatment. An analytical model is introduced to predict the evolution of ambient-temperature yield strength.

Key words: aluminum alloy; Mg; dispersoid strengthening; solid solution strengthening; microstructure characterization; mechanical properties

1 Introduction

AA3xxx aluminum alloys are widely used in packaging, automobile and architecture industries due to their good formability, excellent corrosion resistance and weldability. In general, AA3xxx alloys are considered as non-heat-treatable alloys and the work hardening is the main strengthening mechanism to enhance the mechanical properties. In recent years, the strengthening effect of dispersoids in 3xxx alloys has been discovered [1,2]. Through a proper heat treatment, a reasonable amount of dispersoids precipitated within a suitable range of chemical composition. Several possible kinds of dispersoids in 3xxx alloys were reported in previous works. Al_7Mn [3], $Al_{12}Mn$ [3] and Al_6Mn [4] dispersoids were found in Al–Mn alloys. With the addition of Si, α -AlMnSi [5] and α -Al(MnFe)Si [6–10] dispersoids precipitated with an enhanced rate [5]. In commercial 3xxx alloys, α -Al(MnFe)Si dispersoids are the most common dispersoid phase after precipitation heat treatment. It was reported that α -Al(MnFe)Si dispersoids were partially coherent with Al matrix [1] and they were thermally stable at elevated temperatures [7]. The effect of Mn and the synthetic

effect of Mn and Si on dispersoids and mechanical properties of 3xxx alloys were reported [2,11,12]. The additions of Mn and Si can increase the volume fraction of dispersoids and mechanical properties of 3xxx alloys. However, the effects of Mg on microstructure and mechanical properties of 3xxx alloys by precipitation heat treatment were rarely reported. In the present work, the effect of Mg on microstructure and mechanical properties of 3xxx alloys was investigated. The as-cast and heat-treated microstructures were quantitatively evaluated by optical microscopy and transmission electron microscopy. The microhardness and yield strength at ambient temperature were measured and the strengthening mechanisms of alloys were discussed.

2 Experimental

Five experimental alloys were prepared and the melting was conducted in an electric resistance furnace. The melt was poured and solidified in a preheated steel permanent mold. The chemical compositions of experimental alloys are given in Table 1. The cast ingots were heat-treated at 375 °C for 24 h. After heat treatment, the precipitation behavior of dispersoids was evaluated by electrical conductivity, Vickers

microhardness and yield strength. The compressive yield strength at room temperature was measured using Gleeble 3800 thermomechanical testing unit with a strain rate of 0.001 s^{-1} . In order to measure the area fraction of dispersoid zone and dispersoid free zone (DFZ), the samples were etched by 0.5% HF for 20 s and analyzed under optical microscope (Nikon, Eclipse ME600). A transmission electron microscope (TEM, JEM-2100) operated at 200 kV was used to observe the size and distribution of dispersoids. All the TEM images were taken along [001] zone axis direction of Al matrix. The size and number density of dispersoids were measured using the image analysis software (Clemex PE 4.0) with TEM images. The volume fraction (φ_v) of dispersoids was calculated using Eq. (1) according to the method introduced in Ref. [6].

$$\varphi_v = A_A \frac{K\bar{D}}{K\bar{D}+t} (1 - A_{\text{DFZ}}) \quad (1)$$

where A_A is the area fraction of dispersoid zone; A_{DFZ} is the area fraction of dispersoid free zone; \bar{D} is the average equivalent diameter of dispersoids; t is the TEM foil thickness; K is the shape factor of dispersoids.

Table 1 Chemical compositions of alloys investigated (mass fraction, %)

Alloy	Si	Fe	Mn	Mg	Al
DM0	0.25	0.60	1.20	0	Bal.
DM50	0.25	0.56	1.24	0.47	Bal.
DM100	0.25	0.60	1.24	1.00	Bal.
DM150	0.26	0.60	1.24	1.50	Bal.
DM200	0.27	0.60	1.24	2.02	Bal.

3 Results and discussion

3.1 As-cast and heat-treated microstructures

Figure 1 shows typical as-cast microstructures of experimental alloys. The as-cast microstructure was composed of aluminum dendrite cells and a number of Mn-containing intermetallic particles, which distributed at aluminum dendrite boundaries. The predominant Mn-containing intermetallic phase was identified to be $\text{Al}_6(\text{MnFe})$ in the microstructure. In the Mg-containing alloys, a minor phase of black primary Mg_2Si can be found in the matrix (Fig. 1(b)). Because of lack of Mg in DM0 alloy, no primary Mg_2Si particle was observed. The area fractions of both intermetallic phases in five alloys were quantified by image analysis as shown in Fig. 1(c). The area fractions of primary Mg_2Si and Mn-containing intermetallic particles increase with increasing Mg content.

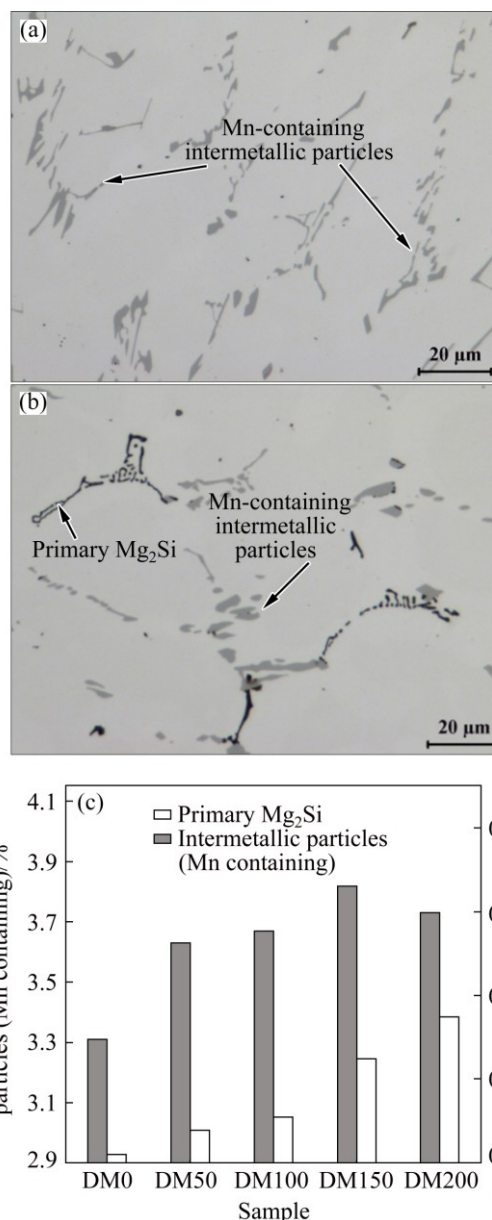


Fig. 1 Typical as-cast microstructures and their area fractions: (a) DM0 alloy; (b) DM100 alloy; (c) Area fractions of primary Mg_2Si and Mn-containing intermetallic particles in five alloys

After heat-treatment at $375 \text{ }^\circ\text{C}$ for 24 h, a number of dispersoids precipitated within aluminum cells/grains while the dispersoid free zone (DFZ) formed in interdendritic regions (Fig. 2). The area fractions of both dispersoid zone and DFZ in the alloys with different Mg contents are shown in Fig. 2(c). For DM0 alloy (without Mg), only a few of dispersoids appeared (Fig. 2(a)) and the dispersoid zone was about 20%. With 0.5% Mg (DM50 alloy), a larger number of dispersoids were observed and the area fraction of the dispersoid zone increased to $\sim 45\%$. When 1.0% Mg was added (DM100 alloy), the area fraction of dispersoid zone continued to increase up to $\sim 70\%$ while the area fraction of the DFZ

sharply decreased to less than 20% (Figs. 2(b) and (c)). With further increasing Mg content in DM150 and DM 200 alloys, the area fraction of dispersoid zone and DFZ remained more or less stable (Fig. 2(c)).

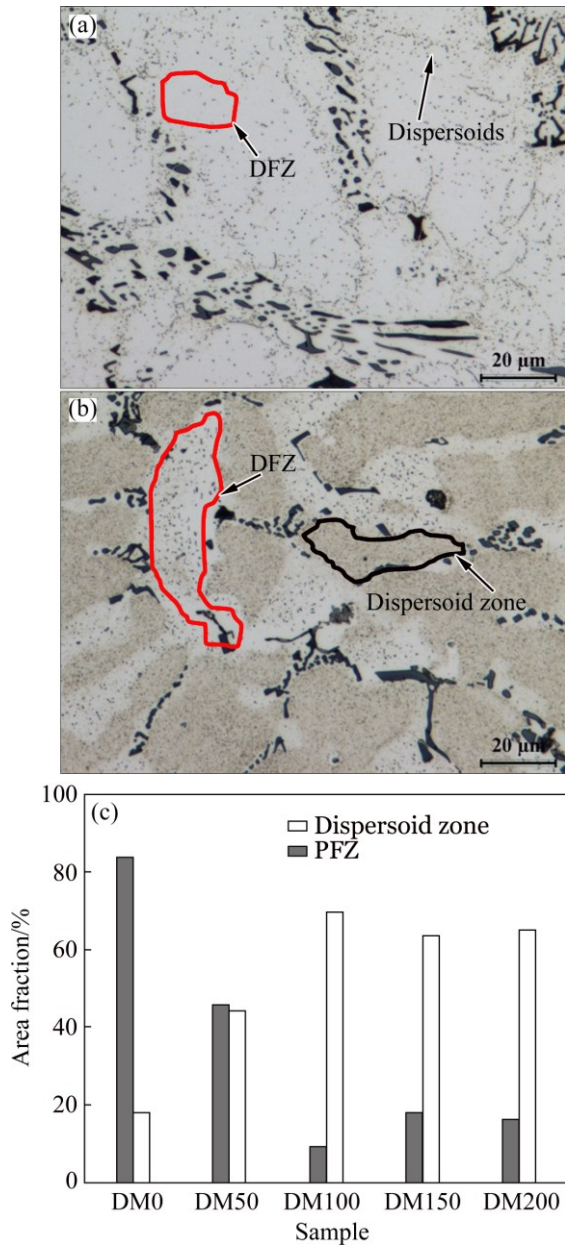


Fig. 2 Distribution of dispersoid zone and DFZ in DM0 alloy (without Mg) (a), DM100 alloy (1.0% Mg) (b) and area fractions of dispersoid zone and DFZ in different alloys (c)

The precipitation of dispersoids is confirmed by TEM observation (Fig. 3). The dispersoids are identified as α -Al(MnFe)Si phase and generally present in two morphologies, cubic or plate-like, and no significant difference in chemical composition is found between two morphologies [1,7,13]. The size, number density and volume fraction of dispersoids in five alloys are shown in Fig. 4. Without Mg (DM0 alloy), the dispersoids seem to be very difficult to precipitate and only few dispersoids

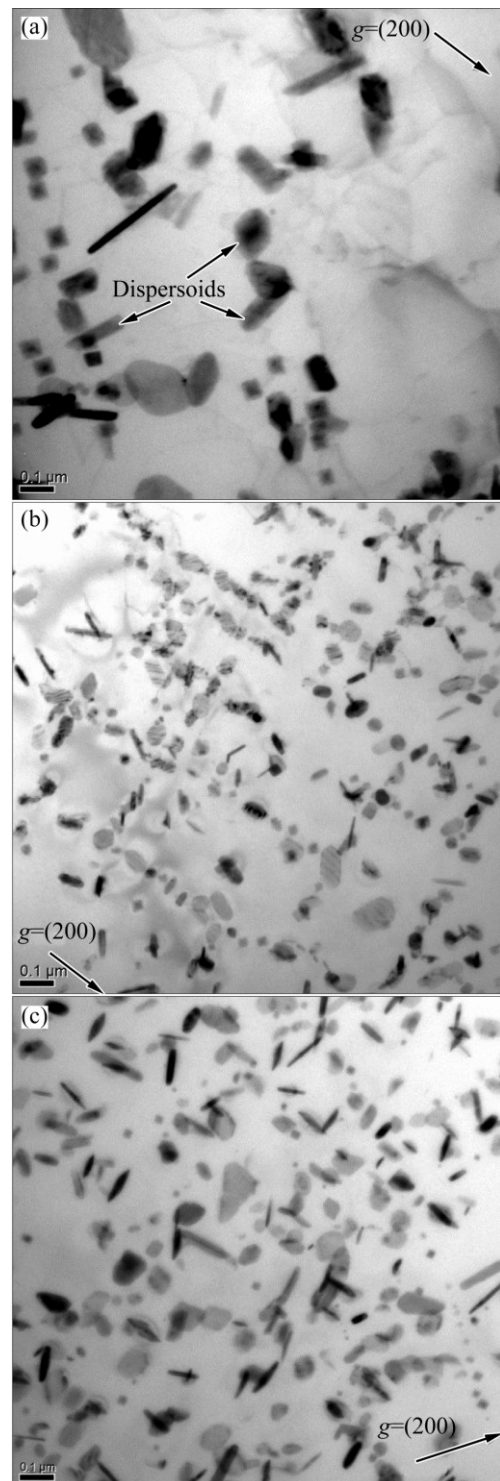


Fig. 3 Precipitation of dispersoids after heat-treatment at 375 °C for 24 h: (a) DM0 (without Mg); (b) DM50 (0.5% Mg); (c) DM100 (1.0% Mg)

with large size (~100 nm) were observed (Fig. 3(a)). With 0.5% Mg addition (DM50 alloy), the number density of dispersoids greatly increases and the size of dispersoids decreases to 45 nm (Figs. 3(b) and 4(a)). With increasing Mg content to 1% (DM100 alloy), the size of the dispersoids slightly increases to 50 nm while

the number density decreases moderately (Figs. 3(c) and 4(a)). With further increasing Mg content to 2%, the number density of dispersoids slightly decreases but the size remains stable around 50 nm (Fig. 4(a)). The volume fraction of dispersoids calculated using Eq. (1) significantly increases from 0 to 1% Mg (Fig. 4(b)). It reaches the maximum value of 2.75% at 1% Mg (DM 100 alloy). For the alloys with 1.5% Mg and 2% Mg (DM150 and DM200 alloys), the volume fraction of dispersoids moderately drops from the peak value (Fig. 4(b)). It is reported that the nano-scale Mg_2Si precipitates can act as the nucleation sites for $\alpha-Al(Mn,Fe)Si$ dispersoids [14]. With the addition of Mg, fine Mg_2Si nanoparticles precipitated at the early stage of the heat treatment process, which provides favorable condition for the nucleation and further precipitation of $\alpha-Al(Mn,Fe)Si$ dispersoids during heat treatment. Because of the lack of Mg and hence no early precipitation of Mg_2Si , the dispersoids in DM0 are difficult to form, and therefore their number density and volume fraction are much lower than those in Mg-containing alloys (Fig. 4). When the Mg content is above 1.0%, the amount of primary Mg_2Si particles increases significantly (Fig. 1(c)) and it considerably decreases the Si level in the solid solution. The available

Si solutes for the formation of $\alpha-Al(Mn,Fe)Si$ dispersoids decrease with increasing Mg content. Consequently, the number density and volume fraction of dispersoids decrease with further increase of Mg content above 1.0%.

3.2 Electrical conductivity and microhardness

To study the precipitation behavior of dispersoids, heat treatments at 375 °C with different holding time were performed on all experimental alloys. The evolution of electrical conductivity (EC, γ) and microhardness is shown in Fig. 5. The EC increases quickly in the first few hours holding and then gradually rises to reach a plateau (Fig. 5(a)). During the heat treatment, for Mg-containing alloys, the continuous decomposition of the supersaturated solid solution and the precipitation of a large amount of $\alpha-Al(Mn,Fe)Si$ dispersoids result in the increase of EC with time. However, for DM0 alloy, the increase of electrical conductivity is mainly due to the decrease of Mn level in the matrix, which leads to the precipitation of some dispersoids and the slight increase of Mn levels in $Al_6(Mn, Fe)$ and $Al(Mn, Fe)Si$ intermetallic particles, as well as the volume fraction of intermetallic particle during the precipitation heat treatment [15].

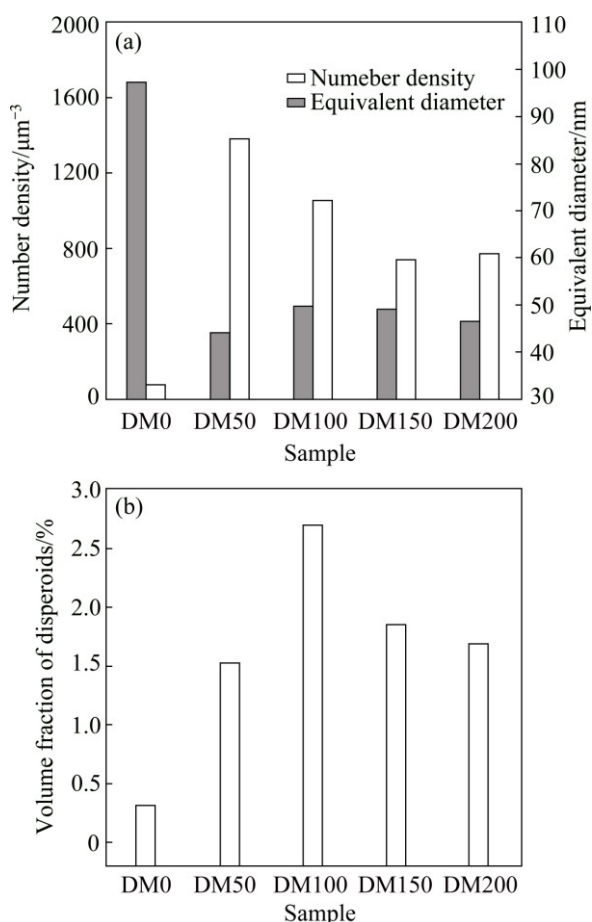


Fig. 4 Distribution of dispersoids in five alloys with different Mg contents: (a) Number density and size; (b) Volume fraction

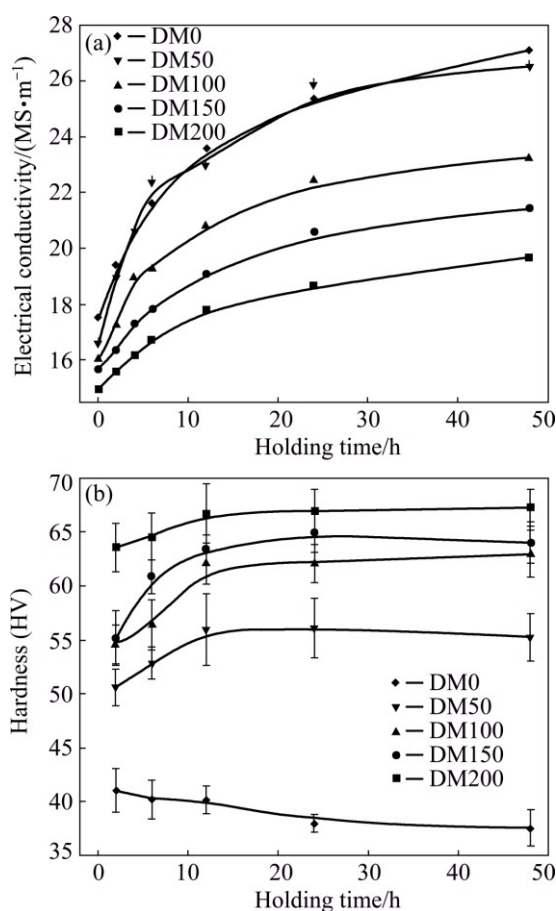


Fig. 5 Evolution of electrical conductivity (a) and microhardness (b) of alloys during heat treatment at 375 °C

The value of EC (γ) can be used to determine the amount of solutes in solid solution using the following equation [6,16]:

$$1/\gamma = 0.0267 + 0.032w(\text{Fe}_{\text{ss}}) + 0.033w(\text{Mn}_{\text{ss}}) + 0.0068w(\text{Si}_{\text{ss}}) + 0.0055w(\text{Mg}_{\text{ss}}) \quad (2)$$

where $w(\text{Fe}_{\text{ss}})$, $w(\text{Mn}_{\text{ss}})$, $w(\text{Si}_{\text{ss}})$ and $w(\text{Mg}_{\text{ss}})$ are mass fractions of individual solutes. As shown in Eq. (2), $w(\text{Si}_{\text{ss}})$ and $w(\text{Mg}_{\text{ss}})$ had much less effect on γ than $w(\text{Mn}_{\text{ss}})$ and $w(\text{Fe}_{\text{ss}})$, but most of Fe was bonded in $\text{Al}_6(\text{MnFe})$ intermetallics during solidification. Therefore, the γ changes during heat treatment are primarily dependent on the soluted Mn in Al matrix and the corresponding amount of Mn solutes in solid solution can be calculated using Eq. (2).

Except DM0 alloy (without Mg), the microhardness of all other alloys increases with the increase of holding time (Fig. 5(b)), indicating the precipitation of dispersoids in Al matrix. The maximum hardness is achieved at 24 h. After that, the microhardness remains quite stable. In general, the microhardness increases with the content of Mg. A slight drop of microhardness in the alloy without Mg during holding also confirms an inadequate dispersoid precipitation, as observed in the metallographic sample.

3.3 Yield strength

The yield strength contribution of alloys by different mechanisms is shown in Fig. 6(a). The measured compressive yield strengths at ambient temperature of experimental alloys are shown in Fig. 6(b). DM0 alloy possesses the lowest yield strength. Compared with DM0 alloy, the yield strength of DM50 alloy (0.5% Mg) increases by more than 20 MPa. With increasing Mg content to 1%, the yield strength keeps increasing until reaching the maximum value of ~100 MPa. A further increase of Mg content up to 2.0% does not bring additional advantage and the yield strength remains at the similar level. The yield strength increment can be attributed to a combination of both dispersoid strengthening and solid solution strengthening. The quantitative analysis will be presented in the following section.

3.4 Mechanisms of strengthening

The results of mechanical properties indicate that the strengths of the alloys are promoted by the precipitation heat treatment at 375 °C but vary with Mg content. In the absence of the traditional precipitation strengthening caused by nano-scale Mg_2Si type precipitates, the strengths of experimental alloys (σ) are mainly contributed by the following three parts: the strength of dispersoid strengthening ($\sigma_{\text{Dispersoids}}$), the strength of solid solution strengthening (σ_{SS}) and the

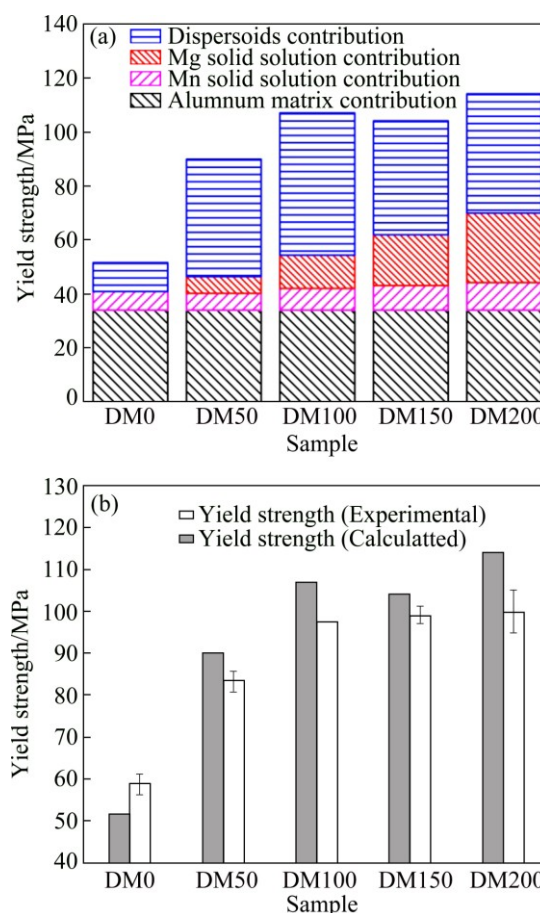


Fig. 6 Yield strength contribution by different mechanisms (a) and comparison between measured and calculated ambient-temperature yield strengths in five alloys with different Mg contents (b)

strength of aluminum matrix (σ_{Al}).

$$\sigma = \sigma_{\text{Dispersoids}} + \sigma_{\text{SS}} + \sigma_{\text{Al}} \quad (3)$$

Because of relatively large size of dispersoids in the present study, the Orowan bowing mechanism can be applied, in which the contribution of dispersoids to the yield strength can be calculated with Ashby–Orowan equation [2]. The data of the size and volume fraction of dispersoids are displayed in Fig. 4.

$$\sigma_{\text{Dispersoids}} = \frac{0.84MGb}{2\pi(1-\nu)^{1/2}\lambda} \ln \frac{r}{b} \quad \text{and} \quad \lambda = r \left(\frac{2\pi}{3f} \right)^{1/2} \quad (4)$$

where M is Talor factor, G is shear modulus of Al matrix, b is Burgers vector, ν is Poisson ratio, λ is interspacing of dispersoids, r is average radius of dispersoids and f is volume fraction of dispersoids. According to Eq. (4), the yield strength increment due to dispersoids increases with increasing volume fraction and decreasing size of dispersoids.

On the other hand, both Mn and Mg solutes in the alloy can also provide solid solution strengthening. The

strength increment, σ_{SS} , due to the solute atoms can be estimated as [17,18]

$$\sigma_{SS}=HC^{\alpha} \quad (5)$$

where C is content of solute atoms, H and α are constants. It is reported in Ref. [19] that $H_{Mg}=13.8$ MPa/%, $\alpha_{Mg}=1$, while $H_{Mn}=18.35$ MPa/% and $\alpha_{Mn}=0.9$ for ambient temperature strength.

As mentioned above, the content of Mn in solid solution can be evaluated using the data of γ and Eq. (2). Because almost no Mg-containing phases are formed during the heat treatment at 375 °C, it is reasonable to assume that except for those bonded in primary Mg_2Si particles, all Mg atoms remain in Al matrix. The calculated results are shown in Table 2.

Table 2 Mg content in solid solution after heat treatment at 375 °C for 24 h

Sample	Area fraction of primary Mg_2Si /%	Mg loss caused by primary Mg_2Si /%	Mg content in solid solution/%
DM0	0	0	0
DM50	0.1	0.05	0.45
DM100	0.24	0.11	0.89
DM150	0.3	0.14	1.36
DM200	0.3	0.14	1.86

For the strength of Al matrix, $\sigma_{Al}=34$ MPa of commercial pure AA1100-O alloy is taken from Ref. [20]. Using the above equations and experimental data, the contribution of dispersoids and solid solutes (Mn and Mg) to the ambient-temperature yield strength can be estimated. Figure 6(a) illustrates the details of each contribution and Fig. 6(b) gives the comparison between theoretical and measured yield strengths of experimental alloys as a function of Mg content. The calculated results are in good agreement with experimentally measured ones, confirming that this analytical model can be used to predict the evolution of ambient-temperature yield strength as a function of alloying element addition. The dispersoid strengthening, promoted by a proper precipitation heat treatment in “non-heat-treatable” 3xxx alloys, is a novel avenue to enhance the alloy strength. Since α -Al(Mn,Fe)Si dispersoids are thermally stable at 300 °C [7], the enhancement of mechanical properties by dispersoid strengthening would be particularly interested for applications at elevated temperatures. The results in Fig. 6(a) also clearly confirm that the dispersoid strengthening plays a predominant role in the strength contribution. The solid solution strengthening of Mn and Mg can also help to improve the strength. However, after the heat treatment, only limited amount of Mn is left in

Al matrix because of the precipitation of Mn-containing α -Al(MnFe)Si dispersoids, and therefore, the strength contribution by Mn solutes is limited. In addition, an excessive addition of Mg increases the amount of large primary Mg_2Si particles and decreases the volume fraction of dispersoids, which may have negative impact on mechanical properties. An appropriate amount of Mg around 1% is suggested to be added.

4 Conclusions

1) Magnesium has a great influence on the volume fraction and distribution of dispersoids in Al–Mn–Mg–Si (3xxx) alloys. With addition of 1% Mg, the maximum volume fraction of dispersoids and minimum volume fraction of dispersoid free zones are obtained during the precipitation heat treatment at 375 °C.

2) The Mg addition into 3xxx alloys improves the yield strength by synthetic effect of dispersoid and solid solution strengthening. The analytical model proposed in the present study can be used to predict the evolution of ambient-temperature yield strength.

3) Dispersoid strengthening is the predominant strengthening mechanism after precipitation heat treatment for Al–Mn–Mg–Si (3xxx) alloys.

Acknowledgment

The authors would like to acknowledge the financial support of the Natural Sciences and Engineering Research Council of Canada (NSERC) and Rio Tinto Aluminum through the NSERC Industry Research Chair in the Metallurgy of Aluminum Transformation at University of Quebec at Chicoutimi.

References

- [1] LI Y J, MUGGERUD A M F, OLSEN A, FURU T. Precipitation of partially coherent α -Al(Mn, Fe)Si dispersoids and their strengthening effect in AA3003 alloy [J]. *Acta Materialia*, 2012, 60: 1004–1014.
- [2] MUGGERUD A M F, MORTSELL E A, LI Y J, HOLMESTAD R. Dispersoid strengthening in AA3xxx alloys with varying Mn and Si content during annealing at low temperatures [J]. *Materials Science and Engineering A*, 2013, 567: 21–28.
- [3] GOEL D B, ROORKEE U P, FURRER P, WARLIMONT H. Precipitation in aluminum manganese (Iron, Copper) alloys [J]. *Aluminium*, 1974, 50: 511–516.
- [4] NICOL A D I. The structure of $MnAl_6$ [J]. *Acta Cryst*, 1953, 6: 285–293.
- [5] HAUSCH G, FURRER P, WARLIMONT H. Recrystallization and precipitation in Al–Mn–Si alloys [J]. *Materials Research and Advanced Techniques*, 1978, 69: 174–180.
- [6] LI Y J, ARBERG L. Quantitative study on the precipitation behavior of dispersoids in DC-cast AA3003 alloy during heating and homogenization [J]. *Acta Materialia*, 2003, 51: 3415–3428.
- [7] LIU K, CHEN X G. Development of Al–Mn–Mg 3004 alloy for applications at elevated temperature via dispersoid strengthening [J]. *Materials and Design*, 2015, 84: 340–350.

- [8] DU Q, LI Y J. Effect modeling of Cr and Zn on microstructure evolution during homogenization heat treatment of AA3xxx alloys [J]. Transactions of Nonferrous Metals Society of China, 2014, 24: 2145–2149.
- [9] WANG N, FLATOY J E, LI Y J, MARTHINSEN K. Evolution in microstructure and mechanical properties during back-annealing of AlMnFeSi alloy [J]. Transactions of Nonferrous Metals Society of China, 2012, 22: 1878–1883.
- [10] HUANG K, LI Y J, MARTHINSEN K. Isothermal annealing of cold-rolled Al–Mn–Fe–Si alloy with different microchemistry states [J]. Transactions of Nonferrous Metals Society of China, 2014, 24: 3840–3847.
- [11] HUANG K, WANG N, LI Y J, MARTHINSEN K. The influence of microchemistry on the softening behaviour of two cold-rolled Al–Mn–Fe–Si alloys [J]. Materials Science and Engineering A, 2014, 601: 86–96.
- [12] HUANG K, ENGLER O, LI Y J, MARTHINSEN K. Evolution in microstructure and properties during non-isothermal annealing of a cold-rolled Al–Mn–Fe–Si alloy with different microchemistry states [J]. Materials Science and Engineering A, 2015, 628: 216–229.
- [13] MUGGERUD A F, LI Y J, HOLMESTAD R. Orientation relationship of dispersoids precipitated in an AA3xxx alloy during annealing at low temperatures [J]. Material Science Forum, 2014, 39: 794–796.
- [14] LODGAARD L, RYUM N. Precipitation of dispersoids containing Mn and/or Cr in Al–Mg–Si alloys [J]. Materials Science and Engineering A, 2000, 283: 144–152.
- [15] DEHMAS M, AEBY-GAUTIER E, ARCHAMBAULT P, SERRIERE M. Interaction between eutectic intermetallic particles and dispersoids in the 3003 aluminum alloy during homogenization treatments [J]. Metallurgical and Materials Transactions A, 2013, 44: 1059–1073.
- [16] OSMAN M M, ENGLER O, KARHAUSEN K, MCLAREN A J. The influence of homogenisation heat treatment on microstructure development in Al–Mg–Mn alloy AA5454 [J]. Materials Science Forum, 2002, 396–402: 351–356.
- [17] SUZUKI T, TAKEUCHI S, YOSHINAGA H. Dislocation dynamics and plastic [M]. Berlin: Springer Verlag, 1991: 32–34.
- [18] RYEN O, NIJS O, SJOLANDER E, HOLMEDAL B, EKSTROM H R, NES E. Strengthening mechanisms in solid solution aluminum alloys [J]. Metallurgical and Materials Transactions A, 2006, 37: 1999–2006.
- [19] HUSKINS E L, CAO B, RAMESH K T. Strengthening mechanisms in an Al–Mg alloy [J]. Materials Science and Engineering A, 2010, 527: 1292–1298.
- [20] KAUFMAN J G. Properties of aluminum alloys: Tensile, creep and fatigue data at high and low temperatures [M]. Washington: ASM International, 1999: 7–16.

镁对 Al–Mn–Mg–Si(3xxx)合金弥散相强化作用的影响

李震, 张展, X-Grant GHEN

Department of Applied Sciences, University of Québec at Chicoutimi,
555 boul. de l'Université, Saguenay, Québec, G7H 2B1, Canada

摘要: 研究 3xxx 系合金中 Mg 对弥散相析出行为和力学性能的影响。通过光学显微镜和透射电子显微镜对铸造组织和热处理后的材料组织进行系统分析。结果显示: 在弥散相析出过程中, 合金中镁含量对弥散相的分布和体积分数有很大影响。室温下显微硬度和屈服强度随着镁含量的增加而增加。对热处理后的材料固溶强化机制和弥散强化机制进行量化分析。在经过热处理后的合金中, 弥散相强化为主要的强化机制。提出了一个数学模型对材料在室温下的屈服强度进行预测。

关键词: 铝合金; 镁; 弥散相强化; 固溶强化; 组织表征; 力学性能

(Edited by Wei-ping CHEN)